

Short communication

Local hydrodynamics in a gas–liquid–solid three-phase bubble column reactor

Wen Jianping ^{*}, Xu Shonglin

Department of Chemical Engineering, Tianjin University, Tianjin 300072, China

Received 23 June 1997; revised 2 November 1997; accepted 19 November 1997

Abstract

A two-dimensional pseudo-two-phase fluid dynamic model with included turbulence model was used to calculate local values of axial liquid velocity and gas holdup in a concurrent gas–liquid–solid three-phase bubble column reactor. The simulated results agreed well with the experimental data. The effects of the solids loading, superficial liquid velocity and superficial gas velocity on the local axial liquid velocity and local gas holdup were experimentally and theoretically examined. © 1998 Elsevier Science S.A. All rights reserved.

Keywords: Bubble column; Hydrodynamics; Three-phase fluidization

1. Introduction

Gas–liquid–solid three-phase bubble columns are presently being used for a wide range of catalytic reactions in both the biochemical and petrochemical industries [1]. The flow patterns of liquid, gas, and solid in these reactors are complex, and the basic principles governing the flow phenomena are not yet fully understood. Detailed experimental and theoretical investigations of local flow characteristics in three-phase reactors, therefore, remain a challenge.

Recently, several papers [2–6] that describe advanced models for two-phase flow in bubble columns have appeared, but relatively little information exists on local flow characteristics of gas–liquid–solid three-phase bubble column reactors [7]. In this paper, a two-dimensional pseudo-two-phase fluid dynamic model with included $k_{\text{sus}}-\varepsilon_{\text{sus}}-k_{\text{b}}-\varepsilon_{\text{b}}$ turbulence model is used to describe and calculate the local flow in a concurrent gas–liquid–solid three-phase bubble column. The effects of solids loading, superficial liquid velocity and superficial gas velocity on local flow characteristics such as axial liquid velocity and gas holdup are reported.

2. Experimental investigations

Measurements were done in a concurrent gas–liquid–solid three-phase bubble column reactor with an inner diameter of

0.29 m and a height of 3.0 m. A sieve plate with evenly spaced 0.1 mm diameter holes was used to sparge the gas phase into the three-phase system. Compressed air was the gas phase. The superficial gas velocity varied from 0.02–0.12 m/s. Tap water was the liquid phase, and the superficial liquid velocity varied from 0–0.08 m/s. The solids used were resin particles of 0.3–0.5 mm with an average density of 1346 kg/m³. The solids loading varied from 0–6% by volume. Sieves at the inlet and outlet of the reactor were used to retain solids. A five-point conductivity probe was used to characterize the local gas holdup and a hot film anemometer was employed for the local axial liquid velocity measurements.

3. Fluid dynamical model

The Eulerian approach was used to describe the flow in gas–liquid–solid three-phase reactor. Based on two-dimensional two-phase fluid dynamic model [3,4], the time-averaged Navier–Stokes equations and the continuity equation were used to develop a two-dimensional pseudo-two-phase fluid dynamic model with included $k_{\text{sus}}-\varepsilon_{\text{sus}}-k_{\text{b}}-\varepsilon_{\text{b}}$ turbulence model. The basic model equations are given in Table 1.

Because the solids loading in three-phase bubble column reactors is usually low, the liquid and solid phase were treated as a pseudo-homogeneous phase, with axially varying density and viscosity. The axial sedimentation dispersion model [8] was used to calculate the axially variation in solids holdup.

^{*} Corresponding author.

Table 1
The governing equations under axisymmetric and steady state conditions

$$(1/r)(\partial/\partial r)(r\rho\alpha\Phi)_k + (\partial/\partial z)(\alpha\rho u\Phi)_k = (1/r)(\partial/\partial r)[r(\mu_c/\sigma)\alpha(\partial\Phi/\partial r)]_k + (\partial/\partial z)[(\mu_c/\sigma)\alpha(\partial\Phi/\partial z)]_k + S_\Phi$$

Equations for	Φ	σ_Φ	S_Φ
Mass	1	∞	$(1/r)(\partial/\partial r)[r\mu_{c,k}(\partial\alpha_k/\partial r)] + (\partial/\partial z)[\mu_{c,k}(\partial\alpha_k/\partial z)]$
Axial-momentum	μ_k	1	$-\alpha_k[(\partial P/\partial z) + \rho_k g] + (1/r)(\partial/\partial r)[r\alpha_k\mu_{c,k}(\partial v_k/\partial z)] + (\partial/\partial z)[\alpha_k\mu_{c,k}(\partial u_k/\partial z)] + (1/r)(\partial/\partial r)[r\mu_k\mu_{c,k}(\partial\alpha_k/\partial z)] + (\partial/\partial z)[\mu_k\mu_{c,k}(\partial v_k/\partial z)] + F_{k,z}$
Radial-momentum	v_k	1	$-\alpha_k(\partial P/\partial r) + F_{k,r} + L_k + (1/r)(\partial/\partial r)[r\alpha_k\mu_{c,k}(\partial v_k/\partial r)] + (\partial/\partial z)[\alpha_k\mu_{c,k}(\partial u_k/\partial r)] - 2\alpha_k\mu_{c,k}(v_k/r)^2 + (1/r)(\partial/\partial r)[r\mu_k\mu_{c,k}(\partial\alpha_k/\partial r)] + (\partial/\partial z)[v_k\mu_{c,k}(\partial\alpha_k/\partial r)]$
Kinetic energy	k_k	1	$\alpha_k(G_k + P_b - \rho_k \epsilon_k)$
Dissipation	ϵ_k	1.3	$\alpha_k(\epsilon_k/k_k)[1.44(G_k + P_b) - 1.92\rho_k \epsilon_k]$

$\mu_{c,k} = \mu_{i,k} + \mu_{lam,k}$, $\mu_{i,k} = 0.09 \rho_k (k^2/\epsilon)_k$.
 k = phase, sus-suspension phase, b-gas phase.
 $G_k = \mu_{i,k} [2 \{ (\partial v_k/\partial r)^2 + (\partial u_k/\partial z)^2 + (v_k/r)^2 \} + (\partial v_k/\partial z)^2 + (\partial u_k/\partial r)^2]$.
 $P_b = 0.7 [F_{sus,z}(u_b - u_{sus}) + F_{sus,r}(v_b - v_{sus})]$.
 $L_b = -L_{sus} = -0.5\alpha_b\alpha_{sus}\rho_{sus}(u_b - u_{sus})\partial u_{sus}/\partial r$.
 $F_{sus,z} = -F_{b,z} = C_W\alpha_{sus}\alpha_b(u_b - u_{sus})$.
 $F_{sus,r} = -F_{b,r} = C_W\alpha_{sus}\alpha_b(v_b - v_{sus})$.

However, note here that the sedimentation dispersion model does not apparently apply to all solid-liquid fluidizations. For example, homogeneous axial distribution of solids in tall bubble columns has been observed by certain authors [9] particularly for low-density solids. The density field of the suspension phase was then calculated using the following equation:

$$\rho_{sus} = \frac{\alpha_l \rho_l + \alpha_s \rho_s}{\alpha_l + \alpha_s} \quad (1)$$

The viscosity of suspension was determined according to Smith [10]:

$$\mu_{sus} = \mu_l \exp \left[\frac{5\alpha_s}{3(1-\alpha_s)} \right] \quad (2)$$

In gas-liquid-solid three-phase system, it is important to model the phase interactions as exactly as possible. Moreover, it is essential to take into account the effect of solids loading on the interfacial drag force. Based on the model by Grienberger and Hoffman [3] for calculating interfacial drag force coefficient, an additional solids dependent factor need to be included. The model could simulate the experimental data when the C_W value was calculated using:

$$C_W = 5 \cdot 10^4 \left(2.2 - 1.7 \sqrt{\frac{r}{R}} \right) (1 - 6\alpha_s) \quad (3)$$

The equations were discretised using a finite volume technique with an upwind or hybrid differencing scheme and solved using a variation of the SIMPLE method and the PEA method.

4. Results and discussion

4.1. Effect of the superficial gas velocity

Figs. 1 and 2 show the effects of superficial gas velocity on the local axial liquid velocity and the local gas holdup at

the same solids loading and superficial liquid velocity. From these figures, the local axial liquid velocity and the local gas holdup increase with increasing superficial gas velocity in a manner similar to that reported in gas-liquid two-phase bubble column [3,11]. Also, the figures show good agreement between the predicted values (solid lines) and the measured data.

4.2. Effect of the superficial liquid velocity

At constant superficial gas velocity and solids loading, an increase in superficial liquid velocity increased the local axial

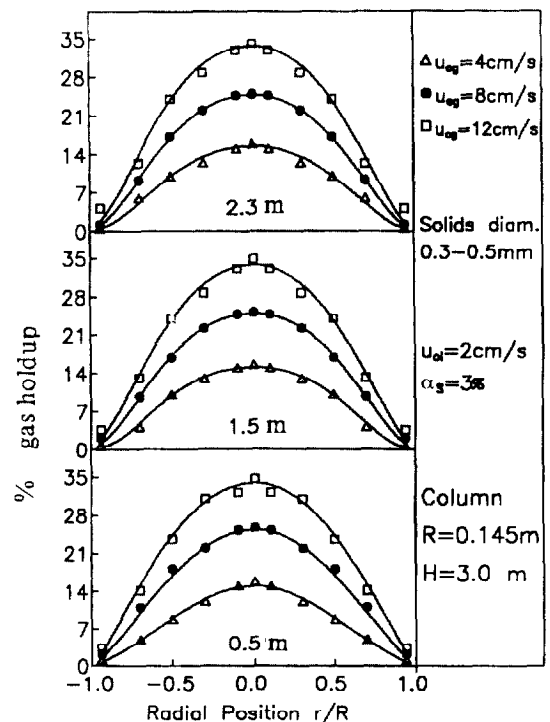


Fig. 1. The effect of superficial gas velocity on local gas holdup.

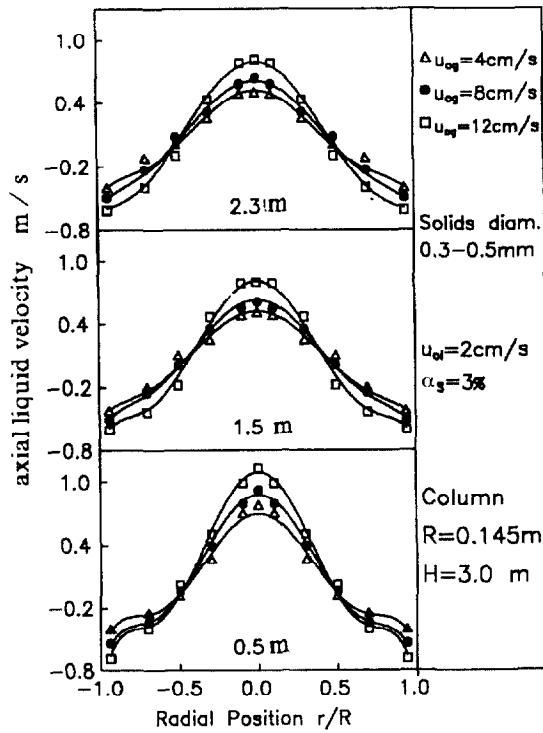


Fig. 2. The effect of superficial gas velocity on local axial liquid velocity.

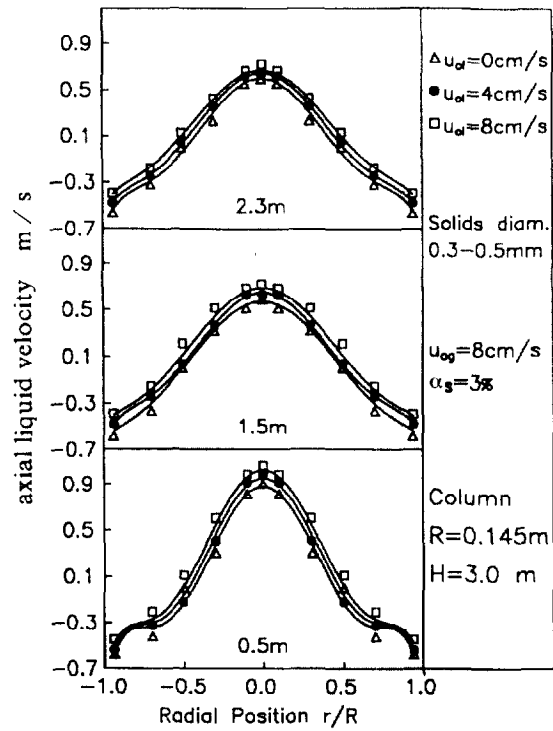


Fig. 4. The effect of superficial liquid velocity on local axial liquid velocity.

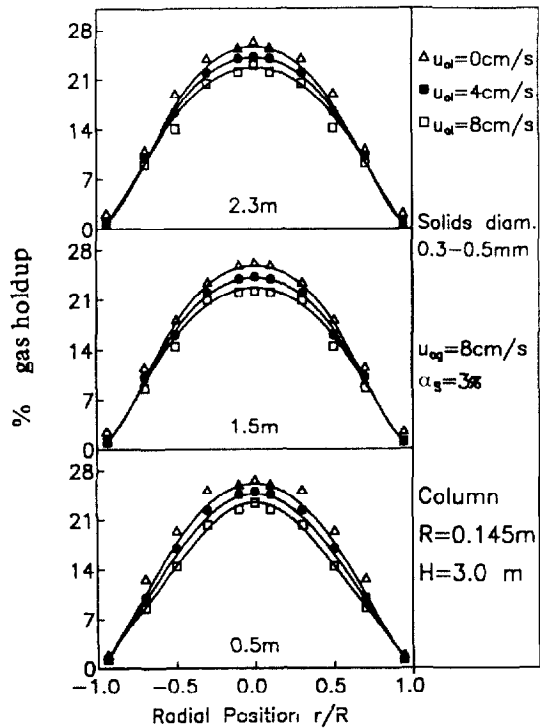


Fig. 3. The effect of superficial liquid velocity on local gas holdup.

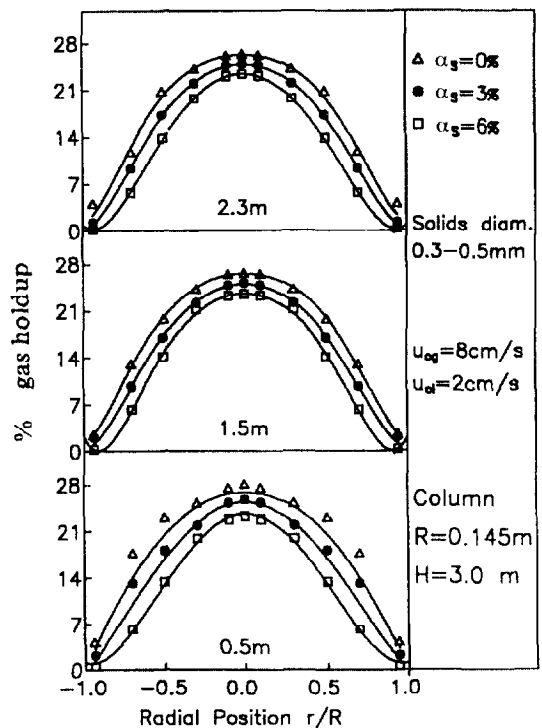


Fig. 5. The effect of solids loading on local gas holdup.

liquid velocity, but the local gas holdup declined (Figs. 3 and 4).

4.3. Effect of the solids loading

The local axial liquid velocity and local gas holdup were also strongly influenced by the amount of solid added to the

gas–liquid two-phase system (Figs. 5 and 6). The solid particles promoted coalescence. Larger bubbles with higher rise velocities were produced, hence, the interfacial drag force reduced, the axial liquid velocity and the gas holdup were reduced relative to the two-phase system.

The model was capable of predicting the influences of superficial liquid velocity and superficial gas velocity on the

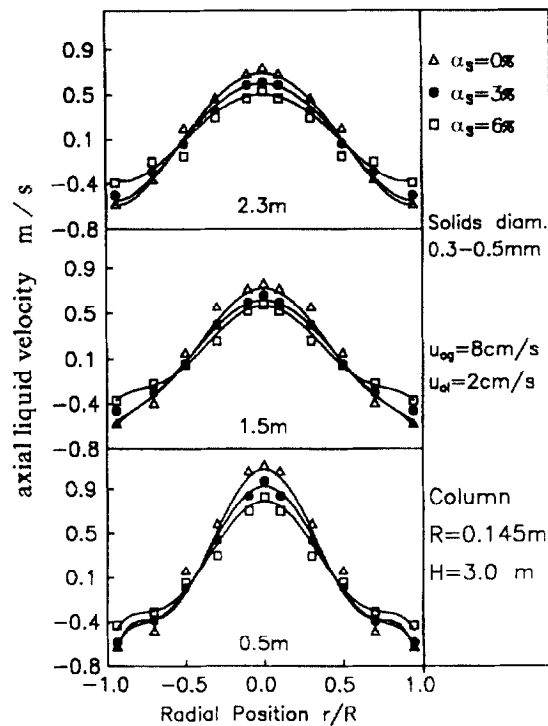


Fig. 6. The effect of solids loading on local axial liquid velocity.

local axial liquid velocity and local gas holdup. In addition, the influence of solids loading on those local flow characteristics could be predicted.

5. Conclusions

A two-dimensional pseudo-two-phase model with included $k_{\text{sus}}-\varepsilon_{\text{sus}}-k_b-\varepsilon_b$ turbulence model was used to simulate the concurrent gas–liquid–solid three-phase bubble column reactor by treating liquid and solid phases as a pseudo-homogeneous phase when the solids loading in three-phase reactors is low. This model was based on the fundamental equations of fluid mechanics. The predicted results of local axial liquid velocity and gas holdup agreed well with the experimental data.

The local axial liquid velocity and the local gas holdup values were strongly influenced by the solids loading and operating conditions. Local gas holdup and axial liquid velocity increased as the solids loading declined. Somewhat unusually, under certain circumstance, the increase in superficial liquid velocity was seen to increase the local axial liquid velocity, and decrease the local gas holdup.

6. Notation

C_m	Constant of radial force, dimensionless
C_w	Interfacial drag coefficient ($\text{kg}/\text{m}^3 \text{ s}$)

F	Friction force ($\text{N}/\text{m}^3 \text{ s}$)
g	Gravitational force (m^2/s)
G	Production of turbulence due to work done by the interaction of the mean flow and turbulent stresses
H	Height of bubble column reactor (m)
k	Turbulent kinetic energy (m^2/s^2)
L	Lateral force, (N/m^3)
P	Pressure (N/m^3)
P_b	Production of turbulence due to work induced by the bubbles
r	Radial position in the bubble column reactor (m)
R	Radius of bubble column reactor (m)
S_{ϕ}	Source terms
u	Axial velocity (m/s)
u_{0g}, u_{0l}	Superficial gas velocity, superficial liquid velocity (m/s)
v	Radial velocity (m/s)
z	Axial coordinate (m)

Greek letters

α	Holdup, dimensionless
ε	Turbulent eddy dissipation (m^2/s^2)
μ	Viscosity (Pa s)
μ_e	Effective viscosity (Pa s)
μ_{sus}	Laminar suspension viscosity (Pa s)
ρ	Density (kg/m^3)
σ	Turbulent Prandtl number, dimensionless
Φ	Variable according to Table 1

Subscripts

b	Gas phase
k	Gas or suspension phase
l	Liquid phase
lam	Laminar
s	Solid phase
sus	Suspension phase
t	Turbulent

References

- [1] L.S. Fan, Gas–liquid–solid fluidization engineering, 1989.
- [2] H.F. Svendsen, H.A. Jakobsen, R. Torvik, Chem. Eng. Sci. 47 (13–14) (1992) 3297.
- [3] J. Grienberger, H. Hofmann, Chem. Eng. Sci. 47 (9–11) (1992) 2215.
- [4] G. Hillmer, L. Weismantel, H. Hofmann, Chem. Eng. Sci. 49 (6) (1994) 837.
- [5] A. Lapin, A. Lubbert, IChemE Symp. Ser. 136 (1994) 365.
- [6] H.E. Gasche, H. Hofmann, Chem. Eng. Technol. 13 (1990) 341.
- [7] S. Grevskott, B.H. Sannas, M.P. Dudukovic, Chem. Eng. Sci. 51 (10) (1996) 1703.
- [8] Y. Kato, A. Nishiwaki, T. Fukuda, S. Tanaka, J. Chem. Eng. Jpn. 5 (1972) 112.
- [9] V. Chisti, Airlift Bioreactors, Elsevier, Amsterdam, 1989.
- [10] O.N. Smith, ACS Symp. Ser. 237 (1984) 125.
- [11] R. Nottenkamper, A. Steiff, P.M. Weinspach, Ger. Chem. Eng. 6 (1983) 147.